AFM Force Measurements between SAM-Modified Tip and SAM-Modified Substrate in Alkaline Solution

Han-Cheol Kwon and Andrew A. Gewirth*

Department of Chemistry and Frederick Seitz Materials Research Laboratory, University of Illinois, Urbana, Illinois 61801

Received: November 23, 2004; In Final Form: March 1, 2005

The reversible desorption and adsorption of ethanethiol (ET) and hexadecane thiol (HDT) self-assembled monolayers (SAMs) on gold substrates are addressed with potential-dependent AFM force measurements where both tip and substrate potentials are controlled independently. For HDT-modified tip and substrate, the potential dependence of the force curve corresponds to the observed voltammetric features. The adhesion interaction between HDT-modified tip and substrate exhibits a large adhesion, whereas the adhesion is reduced to one-quarter of its original value after HDT on the substrate is removed. The presence of both attractive features on the approach curve and large adhesion on retraction after thiol desorption are ascribed to micelle formation from the desorbed, insoluble, thiols above the Au surface. For the ET-modified tip and substrate, the force curve evinces time-dependent recovery after the thiol adsorption peak which arises from the finite time of diffusion of the desorbed thiol back to the substrate. However, the force curves exhibit little potential dependence when the ET-desorbed tip is interacted with ET-modified substrate.

I. Introduction

The ability of atomic force microscopy (AFM) to measure surface forces has been demonstrated in a number of colloidal, biological, and electrochemical systems.[1−4] In particular, the development of AFM and its application in electrochemical systems has significantly advanced our understanding of the microscopic surface phenomena associated with electrochemical events. The application of AFM to electrochemical environments provides a unique view of the electrostatic double-layer and related charge-transfer processes that can be used to measure surface charge quantitatively.[5−10] Tip−surface approach curves have been used to determine the surface charge in the framework of Derjaguin-Landau-Verwey-Overbeek (DLVO) theory, and many important values such as the isoelectric point or point of zero charge have been determined.[9,11−14]

In addition to the approach force curve analysis, adhesion force measurements have received considerable attention. The adhesion measurements can serve as sensitive probes of the variations in the chemical interactions and surface energies and have been extended to pH titration or oxidation-state dependence of the surface.[15−18] For instance, adhesion force measurements have been examined in electrochemical systems and reflects changes in the surface properties of an electrode.[15,16,19] Recently, force measurements using surfaces modified with self-assembled monolayers (SAMs) have become an area of intensive research. In a typical experiment, both the tip and the substrate surface are modified with a functionalized SAM, and the tip−substrate interaction is observed. The tip−substrate adhesion force depends on both the chemical functionality of the tip and the substrate as well as the solvent where the measurements are performed. In this manner, quantitative values such as the surface and interfacial free energy can be determined.[2,20−22]

These monolayer films can be easily prepared by adsorbing the desired thiols on gold and other metal surfaces.[23−25] It is generally accepted that the monolayer formation is initiated by a fast one-electron oxidation step that results in the covalent attachment of the sulfur head to the metallic surface. Then the lateral hydrophobic interactions between adjacent organic chains drive a slow surface rearrangement process to yield the final structure, which consists of densely packed thiol domains. Such surfaces provide good model systems for fundamental studies of wetting, corrosion, or adhesion phenomena, and they represent an important interface between a metal electrode and a biosurface. SAMs can be prepared either by immersing a clean metal in an ethanolic solution of desired thiols[23,26] or by applying a sufficiently positive potential to the metallic substrate in contact with a thiol solution.[27−30] Overall film characteristics such as structures and interfacial properties are essentially identical in both cases, though the deposition conditions can be more compliant with the electrochemical method. These adlayers are stable over a wide potential range, thus opening the possibility to exploit the electrochemical properties of modified electrodes with specific functionalities. The electrochemical properties of SAMs, particularly of alkanethiol SAMs, have been investigated by several groups.[28,31−36]

Although SAMs from alkanethiols resist desorption over a wide potential range, they are desorbed quantitatively at a very negative potential in strong alkaline electrolytes.[27,28,31] Applying a negative potential to the SAM-covered substrate results in a so-called reductive desorption of the thiols in a well-established one-electron reaction. On single crystal surfaces, a typical cyclic voltammetry (CV) exhibits rather sharp cathodic peaks corresponding to stripping of the thiols. The desorption is known to proceed either from a few nucleation centers or nearly homogeneously across the electrode, depending on the chain length of the thiol and the applied potential,[28,31,35] although a report also implicates thiol solubility.[35] The fate of the desorbed

* To whom correspondence should be addressed. Phone: 217-333-8329. Fax: 217-333-2685. E-mail: agewirth@uiuc.edu.

10.1021/jp044655o CCC: $30.25
Published on Web 05/04/2005

thiolates is not clearly understood and has only been observed indirectly.[32,37] In the anodic scan, somewhat broader anodic peaks are observed corresponding to readsorption of the thiols. The readsorption of the thiol can occur through an oxidative process. However, this is strongly dependent on the length of the alkyl chain comprising the thiol. Completely irreversible desorption has been observed for short-chain thiols, whereas a reversible process was noted for thiols of longer chains.[35]

In this paper, we describe potential-dependent force measurements between a SAM-modified AFM tip and a SAM-modified Au substrate. We examine the interfaces of two different electrode surfaces, the SAM-modified and the SAM-desorbed surface, in aqueous electrolyte solution as a function of the applied electrochemical potential. The potential of both tip and substrate are controlled by a bipotentiostat. The force measurements are carried out to simultaneously measure the surface forces and adhesions at the modified electrode surface as the electrochemical potential is varied. Our goal is to apply a combination of interfacial property measurements available with force−distance curve analysis in order to characterize electrochemically induces changes at the SAM-modified surface. Our results show that the change of interaction force during the desorption/adsorption can be related to the voltammetric features. A mechanism for the observed variations in these properties is proposed.

II. Experimental Section

The Au working electrode was prepared by annealing Au coated glass (Dirk Schrõer, Berlin) in a H_2 flame just prior to use.[38] The imaging mode of the AFM was used to position the tip in the center of a large atomically flat crystallite. The Au-coated AFM tip was prepared by depositing 30 Å of chromium and 500∼800 Å of gold successively onto a commercially available Si_3N_4 tip (oxide sharpened, Veeco metrology) using a vacuum evaporator. The tip shape and radius were interrogated by scanning electron microscopy (SEM, Hitachi S-4700), and the typical tip radius after the experiments was measured to be around 150∼180 nm, whereas the tip evinced a pyramidal shape with some roughness apparent at the tip. The cantilever spring constant, k_s, was determined individually, using the method described by Hutter and Bechoffer.[39] We found that tips from the same row within a given wafer exhibited spring constants within ±10% of each other.

A 5 mM solution of ethanethiol (ET; C_2H_6S, Aldrich, 97%) was made using ultrapure water (Millipore Q). 1-Hexadecanethiol (HDT; $C_{16}H_{34}S$, Aldrich, 92%) was dissolved in ethanol. Each SAM-modified Au tip and Au substrate was prepared by immersing it into 10 mL of the desired thiol solution for at least 12 h. Just prior to use, the tip and substrate were taken out of the solution and rinsed with copious amount of ethanol and water to remove any physisorbed thiols. For the ET-modified Au experiment, 0.1 M NaOH (Semiconductor grade, Aldrich) containing 5 mM of ET solution was used as the electrolyte because the cyclic voltammogram is not reproducible without additional thiols in solution (vide infra). For the HDT-modified Au experiment, only a 0.1 M NaOH solution was used as the supporting electrolyte. All solutions were deoxygenated with Ar prior to use for at least for 30 min.

Electrochemical measurements from a Au(111) single crystal (10 mm in diameter, Monocrystal) were performed in the hanging drop configuration using a two-compartment glass cell. The voltammetric data were collected using a gold wire counter electrode and a Ag/AgCl (saturated KCl) reference electrode connected to the electrochemical cell via a capillary salt bridge. The solution in the cell was deaerated with continuous Ar purging during the voltammetric measurement. The Au(111) crystal was flame annealed just prior to use.

For AFM experiments, modified Au substrates were mounted in a small electrochemical cell made of Teflon. Potential control was maintained with a bipotentiostat (AFRDE5, Pine instrument) using a dual working electrode configuration. The first working electrode was the Au substrate, and the second working electrode was the Au-coated AFM tip connected to the bipotentiostat via a wire contacting the Au-coated metal cantilever retaining clip. The counter electrode was a flame annealed Au wire, and the reference electrode was a Ag/AgCl microelectrode (Cypress systems). All potentials reported are reported relative to the Ag/AgCl electrode.

The force measurements were performed in a commercial AFM apparatus (Pico SPM, Molecular Imaging) using commercial control and data acquisition electronics (Nanoscope III, Digital Instruments). The force curves were obtained every 1 s, whereas the substrate potential was scanned at the rate of 5 mV/s with a fixed tip potential. The potential was swept initially to the negative direction (cathodic scan) and then swept back to the original potential. The scan frequency for force measurements of 0.987 Hz was chosen to reduce piezoelement hysteresis. The force data were then converted to force−distance data using well-established procedures.[1,4,40] The cantilever spring constant was used to convert the minimum point in the retraction curve to the adhesion force, whereas the force on the approach curve was measured 5 nm off the surface. The value of 5 nm for measuring the force on approach is arbitrarily chosen because at these distances the electrostatic force is the main interaction experienced by the tip, as the diffuse charge layers of the two surfaces are still overlapped generating an attractive or repulsive interaction while the van der Waals interaction is negligible.[14,19] Each force value was then normalized by dividing the force with the tip radius to give the adhesion force (F_{ad}) and the force on the approach curve (F_{app}). We showed individual force curves for other processes in previous work.[15,16,19]

III. Results

3.1. Voltammetry. Figure 1a shows the CV for HDT desorption/adsorption on Au(111) in 0.1 M NaOH at a scan rate of 5 mV/s. All CVs were initiated at the positive end. The dotted line shows the CV obtained from a Au(111) single crystal in an electrochemical cell with continuous Ar purging, and the solid line shows the CV of Au(111) coated glass in the actual AFM cell. The CV of HDT on Au single crystal exhibits two overlapping waves for both desorption and adsorption. The potential values for desorption are −1.13 and −1.16 V, and those for adsorption are −0.88 and −0.94 V. There has been considerable discussion in the literature regarding the origin of the two peaks found here. These two features are ascribed to either faradaic and capacitive processes due to the formation of micelles[37,41] or the presence of steps on the crystal surface.[28,31] In contrast to the CV of HDT from a Au single crystal, the CV obtained from Au coated glass in the AFM cell exhibits only one wave (solid line in Figure 1a). The desorption and adsorption peaks are found to be −1.12 and −0.88 V, respectively. We note that voltammetry obtained from intentionally roughened surfaces also exhibits only one peak in this region.[31] The CV also exhibits a sloping baseline due to the inevitable presence of oxygen in the open AFM cell.

The CV obtained from a Au(111) single crystal (dotted line) or a Au coated glass substrate (solid line) in 0.1 M NaOH solution containing 5 mM ET is shown in Figure 1b. The CV

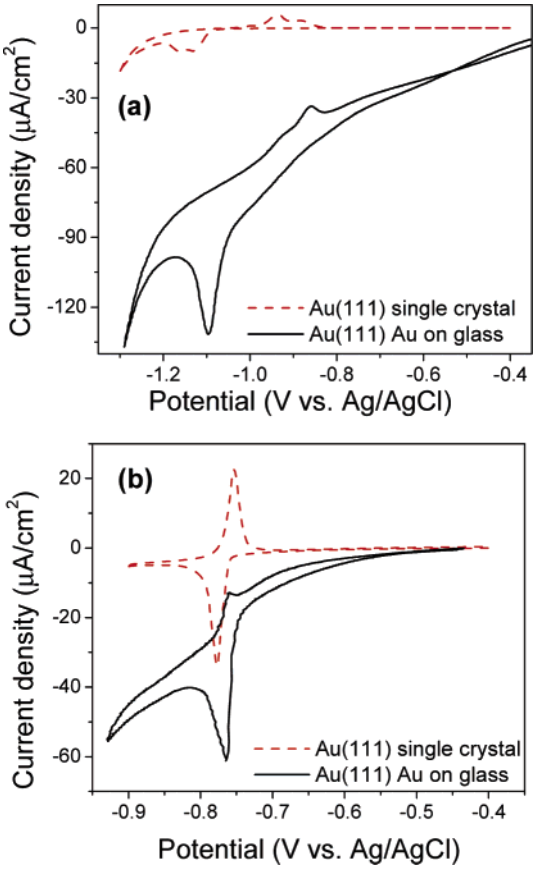

Figure 1. (a) CV for HDT desorption/adsorption on Au(111) in 0.1 M NaOH, and (b) CV for ET on Au(111) in 0.1 M NaOH + 5 mM ET (Dotted line showed the CV in electrochemical cell with Au single crystal, and solid line showed the CV in AFM cell with Au coated glass).

from the Au(111) single crystal exhibits a single desorption/adsorption peak at −0.78 and −0.75 V, respectively, consistent with that reported for slightly longer chain alkanethiols on Au(111) in the alkaline solution.[42] The small difference between the potentials of the reductive and the oxidative current peaks for ET was taken as an indication of a fast and reversible electron transfer.[37] The CV from the Au coated glass in the AFM cell also exhibits a single desorption peak at −0.76 V with a smaller adsorption peak. In addition, this CV also features the sloping baseline arising from the presence of oxygen.

3.2. Force Measurements. *3.2.1. HDT-Modified Au Tip and HDT-Modified Au Substrate.* Figure 2a shows the potential dependence of F_{ad} obtained with the tip potential held at −0.5 V in 0.1 M NaOH solution overlaid with the corresponding CV. The SAM is maintained on the tip at this tip potential. On the cathodic scan, the magnitude of F_{ad} is found to be ca. 350 mN/m, which is comparable to previous measurements of the interaction between CH_3-terminated thiols in aqueous media.[18,43] No changes in F_{ad} are found as the potential of the substrate electrode is scanned between −0.5 and −1.0 V. The voltammetry shows a peak around −1.1 V attributed to the reductive desorption of HDT. As the potential of the substrate is scanned through −1.1 V, F_{ad} starts to decrease and achieves a value of ca. 90 mN/m at −1.3 V. Reversing the potential leads to the relatively low F_{ad} values until a potential of −0.9 V is obtained. Here, the voltammetry exhibits an anodic peak associated with HDT adsorption,[31] and the F_{ad} values returns to the value found on the beginning of the cathodic scan.

Figure 2b shows the potential dependence of F_{app} obtained with the tip potential held at −0.5 V overlaid with the

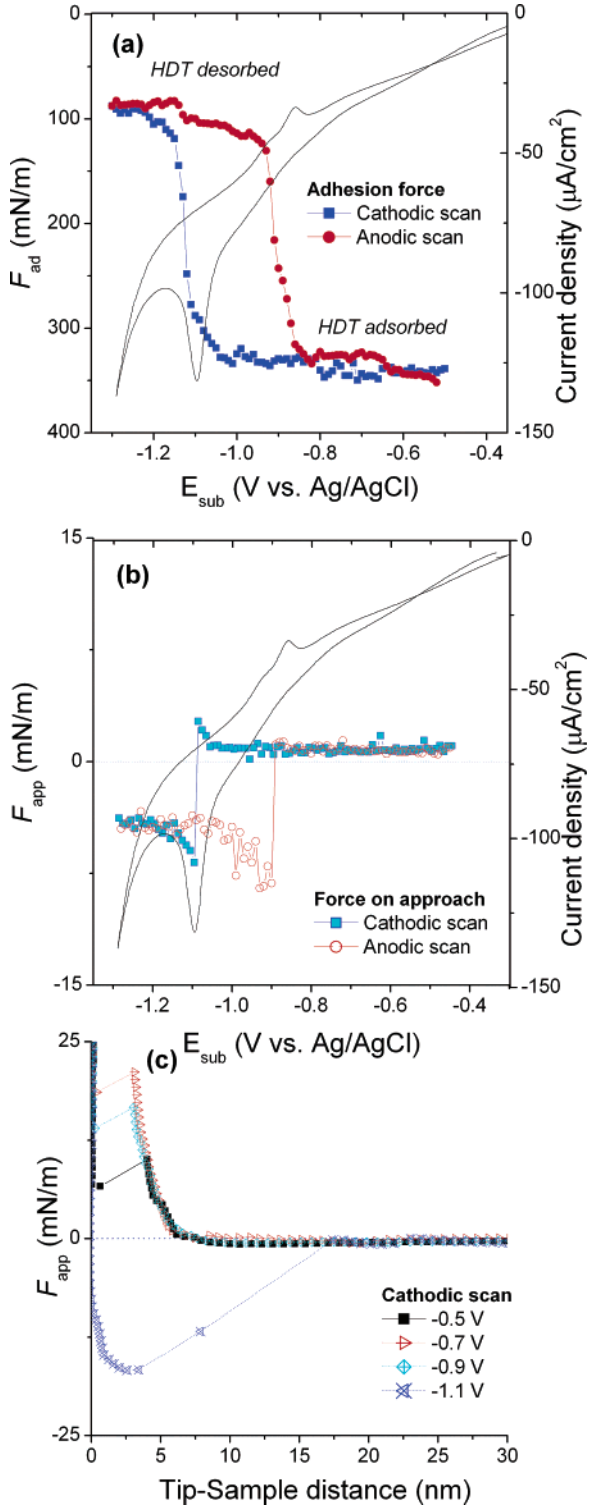

Figure 2. Measurement of (a) adhesion force (F_{ad}) and (b) force on approach (F_{app}) vs applied substrate potential for HDT desorption/adsorption on Au(111) in 0.1 M NaOH (tip potential = −0.5 V). (c) Force−distance curve on approach during electrochemical desorption/adsorption of HDT at given substrate potentials.

corresponding CV. At relatively positive potentials, the tip−sample interaction 5 nm off of the surface is found to be slightly repulsive and is constant until a substrate potential of −1.1 V is reached. Interestingly, the shape of the approach curve just before the region of constant compliance is potential independent for the HDT-HDT case. This behavior is in contrast to the potential-dependent approach force curves obtained by Bard and co-workers using a much more dilute electrolyte and an

TABLE 1: Summary of F_{ad} and W_{ad} in Different Tip/Substrate Potentials

E_{tip} (V)	E_{sub} (V)	tip	substrate	F_{ad} (mN/m)	W_{ad} (mJ/m^2)
−0.5	−0.5	HDT	HDT	368 ± 20	78 ± 4
−0.5	−1.3	HDT	HDT-desorbed	90 ± 22	19 ± 4
−1.2	−0.5	HDT-desorbed	HDT	89 ± 34	21 ± 6
−1.2	−1.3	HDT-desorbed	HDT-desorbed	27 ± 4	6 ± 1
−0.4	−0.4	ET	ET	314 ± 30	67 ± 6
−0.4	−0.9	ET	ET-desorbed	28 ± 10	6 ± 2
−0.9	−0.4	ET-desorbed	ET	17 ± 4	4 ± 1
−0.9	−0.9	ET-desorbed	ET-desorbed	2.7 ± 1.1	0.6 ± 0.2
−0.5	−0.5	bare Au	bare Au	1.7 ± 0.5	0.4 ± 0.1

insulating tip.[6] At a potential of −1.1 V, corresponding to desorption of HDT from the Au substrate surface, the tip−sample interaction becomes attractive and is maintained at these negative potentials until the potential of thiol readsorption is reached on the anodic scan. Close examination of the force curve on approach shows that the attractive interaction is a result of a jump-to-contact occurring at ca. 15 nm from the surface as shown in Figure 2c. However, at ca. 3 nm away from the surface, the force curve exhibits some structure before the region of constant compliance. Moving the potential to more positive values makes F_{app} repulsive again with about the same value as found before the desorption.

3.2.2. Calculation of Work of Adhesion. The average adhesion force for SAM-modified tips depends on the surface energies of the SAMs; that is, F_{ad} between the AFM tip and the substrate surface can be related to the work of adhesion (W_{ad}) using Johnson-Kendall-Roberts (JKR) theory.[20,21] In this model, F_{ad} is proportional to W_{ad} needed to separate the tip and substrate's surfaces

$$F_{ad} = 1.5\pi W_{ad} \quad (1)$$

In addition, W_{ad} can be expressed in surface free energy by Dupré equation[1,20]

$$W_{ad} = \gamma_{13} + \gamma_{23} - \gamma_{12} \quad (2)$$

where γ_{13} is the tip surface free energy in equilibrium with the medium, γ_{23} is the substrate surface free energy in equilibrium with the medium, and γ_{12} is the interfacial free energy of the tip−substrate contact interface. For identically functionalized tip−substrate combination, e.g. CH_3−CH_3, the work of adhesion is $W_{ad} \approx 2\gamma$, where $\gamma = \gamma_{13} = \gamma_{23}$ is the surface free energy of the particular surface functionality against the medium, the interfacial free energy γ_{12} between the same bulk material being negligible.[21,44]

To calculate the tip−substrate interaction energy, multiple force curves were collected and averaged with all possible tip−substrate combinations. For example, when the tip and substrate were held at −0.5 V so that the HDT was retained in both surface, measured F_{ad} was 368 ± 20 mN/m. W_{ad} for the CH_3−CH_3 interaction was then calculated to be 78 ± 4 mJ/m^2, which is somewhat smaller than the literature value of ∼103 mJ/m^2.[20,22,45] The large variation and rather low adhesion forces may be attributed to the surface heterogeneity of both tip and substrate used in this work, since SEM images (not shown) reveal a rough tip following Au deposition onto it.[18,43] Table 1 shows the obtained F_{ad} (and W_{ad}) for all measurement results.

3.2.3. Bare Au Tip and HDT-Modified Au Substrate. To monitor the interaction between a bare Au tip and the HDT-modified Au substrate, the tip potential was held at −1.2 V so that HDT was desorbed from the Au tip. Figure 3a shows the potential dependence of F_{ad} with the tip potential held at −1.2 V in 0.1 M NaOH solution. At relatively positive potentials, F_{ad} exhibits values of 89 ± 34 mN/m, which is comparable to that found between the HDT-modified Au tip and HDT-desorbed Au substrate, described above. The adhesion force is found to decrease as the potential of HDT desorption from the substrate is passed on the cathodic scan, yielding a value of 27 ± 4 mN/m. Upon reversing the potential scan direction, thiol readsorption to the substrate at −0.9 V is accompanied by a sharp increase in F_{ad}, which then returns to the value found at the beginning of the cycle.

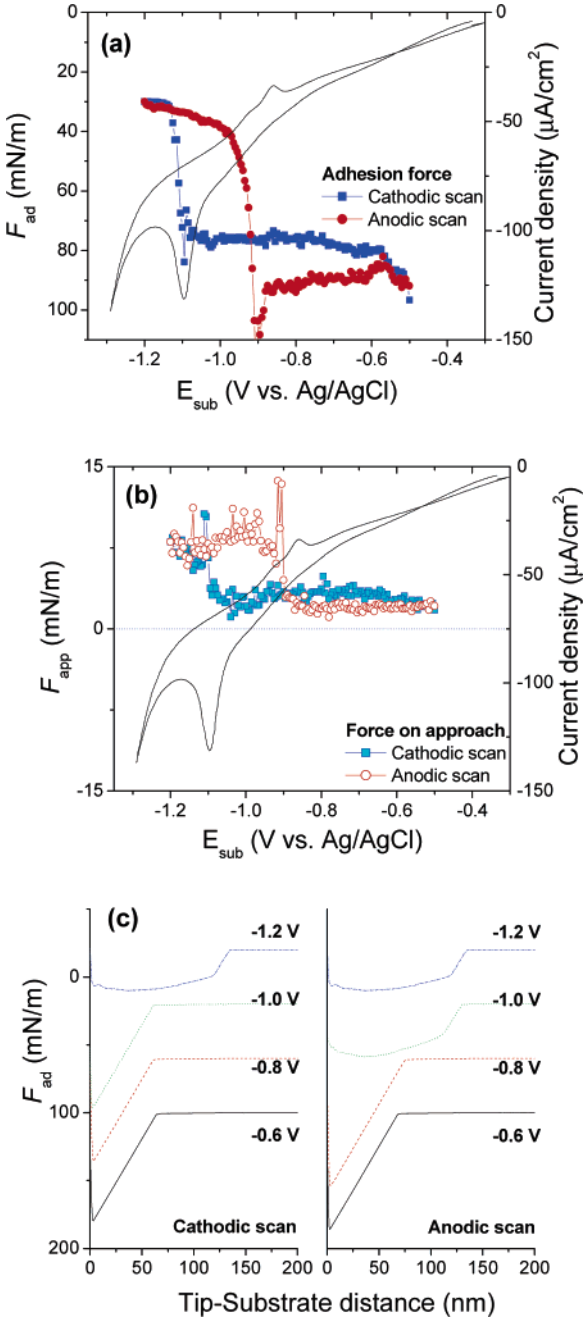

Figure 3. Measurement of (a) adhesion force (F_{ad}) and (b) force on approach (F_{app}) vs applied substrate potential for HDT desorption/adsorption on Au(111) in 0.1 M NaOH (tip potential = −1.2 V). (c) Force−distance curve on retraction during electrochemical desorption/adsorption of HDT at different substrate potentials. Each curve was offset for clarity.

Figure 3b shows the potential dependence of F_{app} obtained at a tip potential of −1.2 V overlaid with the corresponding CV. The plot shows that F_{app} follows the CV as before. At the beginning of the cycle at −0.4 V, F_{app} is low and repulsive as

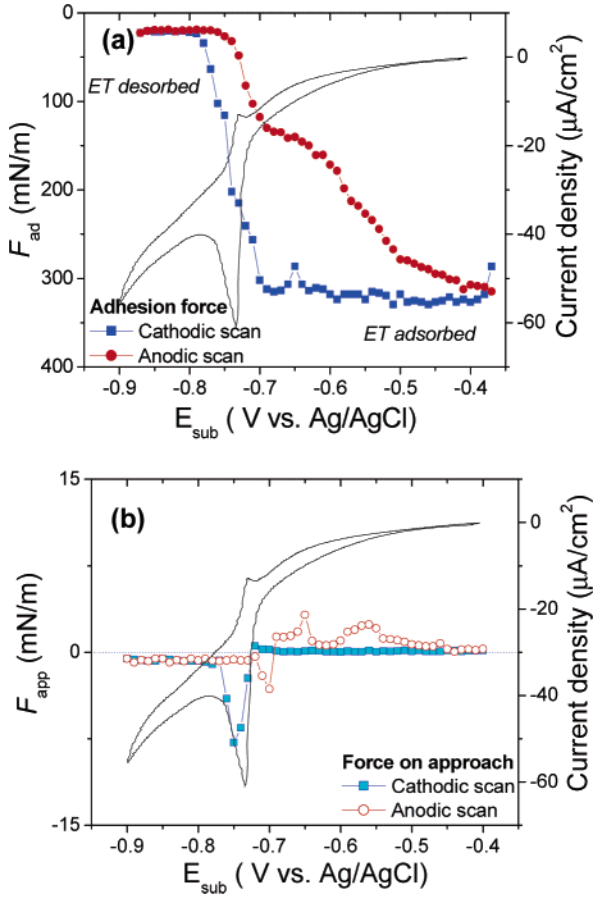

Figure 4. Measurement of (a) adhesion force (F_{ad}) and (b) force on approach (F_{app}) vs applied substrate potential for ET desorption/adsorption on Au(111) in 0.1 M NaOH + 5 mM ET (tip potential = −0.4 V).

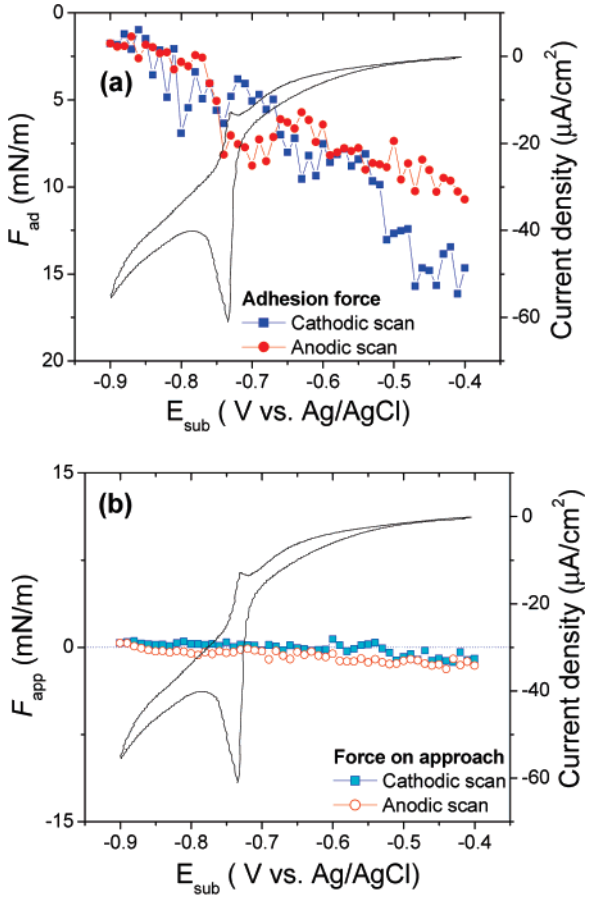

Figure 5. Measurement of (a) adhesion force (F_{ad}) and (b) force on approach (F_{app}) vs applied substrate potential for ET desorption/adsorption on Au(111) in 0.1 M NaOH + 5 mM ET (tip potential = −0.9 V).

found previously. However, after passing −1.1 V and desorption of thiol from the substrate, F_{app} becomes more repulsive and essentially remains so until thiol readsorption on the substrate at −0.9 V on the anodic scan. This behavior is in contrast to that found above with the thiol-adsorbed tip where F_{app} became attractive with following thiol desorption from the substrate.

Figure 3c shows the actual force−distance curves obtained by the tip retraction (monitoring adhesion) during electrochemical desorption/adsorption with the tip potential held at −1.2 V. At potentials positive of the desorption peak, the force curve exhibits a sharp break at distances less than 5 nm as the tip is pulled away from the surface. When the substrate potential is negative of the desorption peak, the retraction force curves do not exhibit a sharp break, but rather show an adhesive component extending up to 100 nm off the surface. However, as the potential is swept back to more positive values, and the thiol adlayer reforms on the Au surface, the retraction force curves again recovers the behavior seen prior to thiol adlayer desorption.

3.2.4. ET-Modified Au Tip and ET-Modified Au Substrate. To evaluate differences between alkanethiols with different chain lengths, we examined the ethanethiol (ET)-modified Au system. Figure 4a shows the potential dependence of F_{ad} obtained with the tip potential held at −0.4 V in a solution consisting of 0.1 M NaOH + 5 mM ET overlaid with the corresponding CV. At this tip potential, the tip surface is covered with ET. At positive substrate potentials, the measured F_{ad} is found to be large, reaching a value of 314 ± 30 mN/m. As the substrate potential is scanned in the negative direction, F_{ad} starts to decrease at −0.7 V, just at the onset of the desorption wave in the voltammetry. When the substrate potential reaches −0.9 V, F_{ad} is fairly small. In the anodic scan, F_{ad} starts to increase after passing the anodic peak, but in contrast to the HDT case, F_{ad} does not reach its initial value until nearly at the positive potential limit. In force curves obtained with different potential scan rates, the potential dependence of F_{ad} recovery was always slower than that found with HDT.

Figure 4b shows the potential dependence of F_{app} obtained under the same conditions described above. With both the tip and the substrate covered with ET, F_{app} 5 nm off the surface is nearly zero. At the potentials where ET is desorbed from the substrate, between −0.7 and −0.75 V, F_{app} is found to be attractive before again approaching zero. On the anodic scan, F_{app} becomes unstable, exhibiting both repulsive and attractive values until ET SAM reformation is completed at ca. −0.4 V.

3.2.5. Bare Au Tip and ET-Modified Au Substrate. Figure 5a shows the potential dependence of F_{ad} obtained from an ET-modified Au substrate with the tip potential held at −0.9 V under the conditions described in the previous section. In contrast to the previous cases reported above, the F_{ad} curves shown here exhibit only weak potential dependence. Additionally, F_{ad} is found to be quite low. At the initial substrate potential of −0.4 V, F_{ad} is 17 ± 4 mN/m, and this value decreases to being negligible (2.7 ± 1.1 mN/m) at −0.9 V. Reversing the scan direction results in the gradual reestablishment of F_{ad}. Although some combinations of certain tips and substrates exhibited weak potential-dependence associated with the voltammetry, most cases exhibited a linear change in F_{ad}.

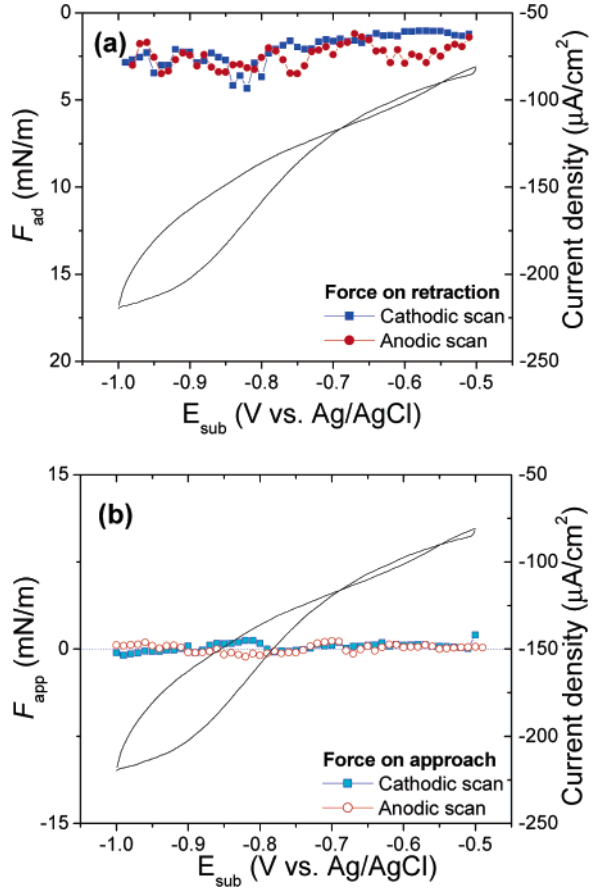

Figure 6. Measurement of (a) adhesion force (F_{ad}) and (b) force on approach (F_{app}) vs applied substrate potential for bare Au(111) in 0.1 M NaOH (tip potential = −0.5 V).

Figure 5b shows the potential dependence of F_{app} obtained with the tip potential held at −0.9 V overlaid with the corresponding CV. The figure shows that F_{app} is essentially zero throughout the entire potential range examined in this experiment. Additionally, examination of the force curves shows that the jump-to-contact, seen at ca. 2∼3 nm in all the cases discussed above, is absent in the force curves obtained with the tip potential held at −0.9 V.

3.2.6. Bare Au Substrate and Bare Au Tip. Figure 6a shows the potential dependence of F_{ad} obtained from a bare Au substrate and a bare Au tip in a solution containing 0.1 M NaOH with the tip potential held at −0.5 V. This potential dependence is overlaid with the Au(111) voltammetry obtained in the AFM cell. In previous work utilizing single crystals, the voltammetry in this potential region was found to be featureless, since oxide formation occurs some at 0.6∼0.7 V more positive potentials.[46,47] The voltammetry presented here exhibits a sloping baseline due to the presence of oxygen. With a bare tip and sample, F_{ad} is nearly potential independent, as was found previously for a Si−O− functionalized tip and an Au surface in this electrolyte.[16]

Figure 6b shows the potential dependence of F_{app} obtained with a tip potential of −0.5 V overlaid with the corresponding CV. The plot also shows that F_{app} is almost zero 5 nm off the surface and potential independent. Examination of the force curves shows that the repulsion force is always present and the jump-to-contact is absent throughout the entire potential region, consistent with previous results.[16] The small repulsion is a consequence of the intermediate electrolyte concentration giving rise to a Debye length of less than 1 nm.[1] The effect of this collapsed double layer has been seen in measurements of

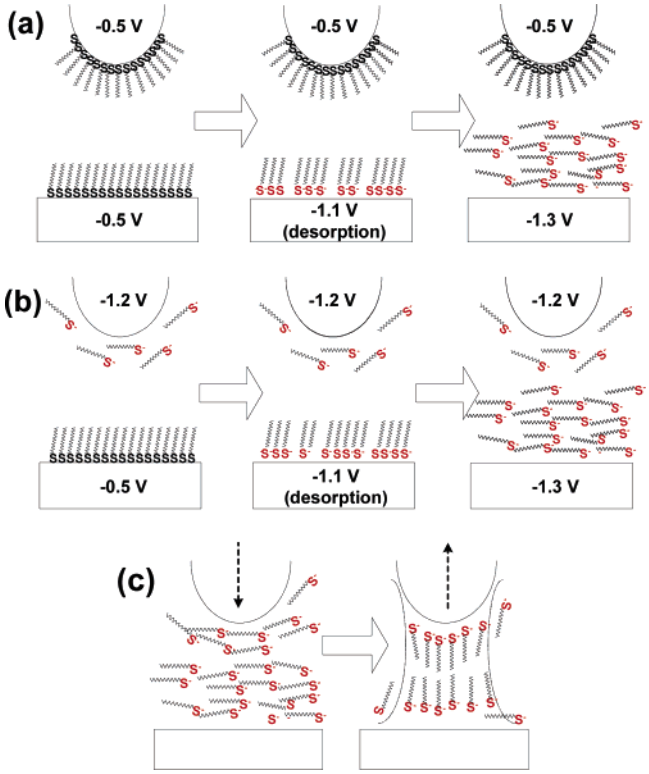

Figure 7. Schematic diagram for HDT-modified tip and HDT-modified substrate during the desorption/adsorption cycle. (a) The tip potential is held at −0.5 V (HDT-covered tip) and (b) the tip potential is held at −1.2 V (bare Au tip). (c) Model for long-range attraction during retraction when both tip and substrate is free of HDT (Tip potential and substrate potential is held at −1.2 V).

repulsive force as a function of electrolyte concentration, which show at intermediate (0.1 M) salt concentrations, that the repulsive component in the force curve has effectively been removed.[48] However, as the electrolyte concentration is increased beyond 0.1 M to 1 M or higher, a repulsive interaction is again observed.[49,50]

IV. Discussion

The results presented above show that the tip−substrate interaction is a sensitive function of the chemistry of both the tip and the substrate, and that this interaction also exhibits considerable potential dependence. We show by changing the alkanethiol chain length that remarkably different interaction behaviors are obtained. In what follows, we discuss (a) potential dependence of HDT-modified Au substrate, (b) potential dependence of ET-modified Au substrate, and (c) differences between the different thiol chain lengths. Figures 7 and 8 provide a schematic explanation of the observed behaviors.

4.1. HDT-Modified Tip and Substrate. *4.1.1. Adhesion Measurements.* Interaction of a thiol-modified Au substrate with a thiol-modified AFM tip showed a large F_{ad} when the thiols were maintained on the AFM tip. The magnitude of W_{ad} for HDT−HDT interaction was found to be 78 ± 4 mJ/m^2 on the beginning of the cathodic scan and this magnitude was regained after a full potential cycle, as shown in Figure 2a. However, when the thiol was desorbed from the substrate by moving the potential to negative values, W_{ad} changed to a value of 19 ± 4 mJ/m^2. This change was reversible and reproducible. As described above, W_{ad} for the CH_3-CH_3 contact is at the magnitude expected from previous work. Clearly, the adhesive interaction changes between a CH_3-CH_3 contact and a CH_3-(thiol desorbed) contact.

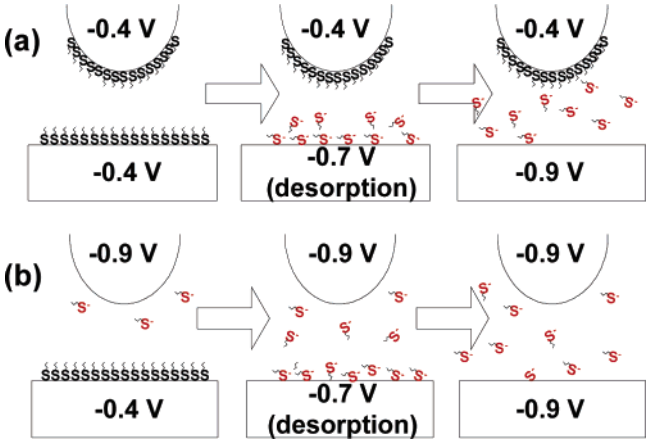

Figure 8. Schematic diagram for ET-modified tip and ET-modified substrate during the desorption/adsorption cycle. (a) The tip potential is held at −0.4 V (ET-covered tip) and (b) the tip potential is held at −0.9 V (bare Au tip).

Interestingly, W_{ad} for the HDT-modified tip and the HDT-desorbed substrate did not go to zero but rather dropped to about one-fourth of its initial value. This suggests that there are still CH_3−alkane interactions available in the tip−substrate contact area. HDT is not soluble in aqueous solution, and it is thought that aggregates of desorbed thiolates are formed and sustained near the substrate after reduction.[35,37] The interaction between these aggregates and the HDT-modified tip likely gives rise to the finite W_{ad} values.

A manifestation of this behavior is found in the HDT-desorbed tip/substrate measurements shown in Figure 3a. Here, with the HDT-desorbed tip and the HDT-modified substrate, W_{ad} is comparable to that found with the thiol-modified tip and the thiol-desorbed substrate shown in Figure 2a (i.e., ca. 20 mJ/m^2). However, as the substrate potential is moved to negative values and the thiol is desorbed from the substrate, F_{ad} and consequently W_{ad} decrease to a value now only below 10% of that found for the CH_3−CH_3 case. The nonzero value of W_{ad} suggests that there still exist interactions between desorbed thiol layers, otherwise the bare Au−Au interaction would exhibit a negligible W_{ad}. Parenthetically, we note that the Au−Au adhesive interaction shown in Figure 6a is barely distinguishable from zero at these negative potentials. The 10% value indicates the presence of some alkanethiolates near the interface.

Retraction force curves in the case of a thiol-modified tip and a substrate with or without thiol or a thiol-modified substrate and a tip with or without thiol did not exhibit any long-range interactions, with the tip−sample force going to zero at distances no greater than 60 or 70 nm after pull off. However, as shown in Figure 3c, the HDT-desorbed tip interacted with the HDT-desorbed substrate over very long ranges, up to ca. 150 nm, when the tip was removed from the substrate. The origin of this long-range interaction found on retraction must be the interaction of the micellular, desorbed HDT with the bare Au surface presented by both the tip and the sample. This interaction is not present when the tip is covered with thiols, which indicates that the desorbed thiolates interact with Au much more readily than with thiol itself. This occurrence suggests the formation of a bridge between tip and substrate with thiolate micellular aggregates. When the tip is contacted to the substrate and then removed from the substrate, the desorbed thiolates are pulled between the tip and the substrate because the thiolates are not soluble in bulk solution. A cartoon describing this situation is presented in Figure 7c.

4.1.2. Force Curves on Approach. When the tip and the substrate were both covered with HDT and both held at −0.5 V, the interaction between the two on approach exhibited only a repulsive component at short distance as the tip approached the substrate as shown in Figure 2b. The magnitude of this interaction remained constant throughout the potential range where both the tip and the sample were covered with HDT, which suggests that this interaction is not due to the applied potential. The jump-to-contact distance was ∼4 nm, which is comparable to twice the length scale of HDT on the Au substrate. This suggests that when the HDT layers on both the tip and the sample come together and contact each other the interaction between them is attractive, likely due to a hydrophobic effect.

The origin of the repulsive interaction on approach at distances longer than ca. 4 nm likely is a result of the high pH used in this study. At lower pH, this repulsive component was not observed.[51,52] Additionally, Freitas et al. showed that the interaction between two hydrophobic surfaces was dominated by the long-range attraction due to the hydrophobic force in aqueous solutions but was found to be sensitive to the pH and electrolyte concentration.[53] These authors showed that the interaction between two hydrophobic surfaces presented a repulsive force curve with a large surface potential at high pH. Although the origin of the strong repulsion is not clear, our force curves exhibit similar behavior. This suggests that the surface charge is not completely blocked.

We next address the potential insensitivity of the approach curves for the HDT−HDT case. Previous theoretical work showed that ca. 90% of the applied potential would be dropped within the alkanethiolate adlayer as long as the electrolyte does not penetrate the film.[54] Additionally, impedance measurements showed that alkanethiol adlayers behave as ionic insulators until a critical potential value (V_c) is reached.[55] V_c is associated with the formation of potential-induced surface defects, the potential for which depends on the electrolyte. At potentials more negative than V_c, ionic penetration takes place and the substrate is no longer an ionic insulator.[56] The insensitivity of the repulsive interaction to potential for the HDT−HDT case reported here strongly suggests that the HDT adlayer behaves as an insulator. Additionally, the concentration of the electrolyte is such that little potential dependence is found, even for the bare Au-bare Au case, as described above.

As the substrate potential moves through the desorption peak, the repulsive force increased slightly just before desorption occurred. As the thiol desorbs from the substrate, the tip−substrate interaction becomes instantaneously attractive. At this point, the force curve on approach exhibited a long-range jump to contact starting ca. 10 nm off the surface. The long-range nature of the interaction suggests that species in solution are responsible for the effect. In particular, desorption of the thiol leads to the formation of insoluble thiolates in the region near the substrate surface.[35,37] We suggest that this layer of thiolates contributes to the jump to contact interaction found on approach.

There is considerable evidence for the formation of a disordered thiolate layer in the interfacial region following HDT desorption. In situ vibrational spectroscopy showed an increase in the intensity of the methylene CH stretch following thiol reduction,[37,57] which was attributed to the formation of thiolates micelles. STM imaging revealed that HDT aggregates remained on the Au substrate after reduction and that the monolayer partially recovered upon the oxidative adsorption.[35] However, these results do not provide information about the extent of the micellular structure.

How could the presence of a thiolate micelle at the interface move the jump-to-contact from ca. 4 to 15 nm? If the desorbed thiolate interacted with the HDT remaining on the tip, possibly because of a hydrophobic interaction, then the presence of the thiol on the tip could cause organization to occur in the thiolate near the substrate. Indeed, the force curve shown in Figure 2c shows the presence of an additional structure in the repulsive region after the jump-to-contact which could likely be the result of further thiolate organization.

Upon the anodic scan, the force on approach remained attractive at negative potentials until the thiolates adsorbed again onto the Au substrate surface. F_{app} became repulsive immediately and exhibited the same value as found before the occurrence of HDT desorption. This shows that the thiol layer reforms on the substrate, as expected.[49,50]

The interaction on approach between the HDT-desorbed Au tip and the HDT-modified Au substrate exhibited a different potential dependence, as shown in Figure 3b. At positive substrate potentials where the tip is bare and the surface is covered with thiol, the interaction on approach was repulsive. Interestingly, the parallel situation reported above (thiol-covered tip/thiol-desorbed substrate at −1.3 V) exhibited an attractive interaction. The contrast between the two situations likely originates from the different amounts of thiolate in the interfacial region between the tip and the substrate. In this case, there is relatively little thiolate because of the smaller tip area in the interaction region. The negatively charged, bare Au tip would then exhibit a repulsive interaction with the somewhat negatively charged, thiol-covered Au substrate (Au-thiol pzc = −0.17 V in ethanolic KOH[30]). This interaction is apparently not screened as much as is found for the bare Au−bare Au case. One possible origin of the increased repulsive interaction would be the presence of small amounts of desorbed HDT from the tip in the interfacial region. However, the exact mechanism of this repulsive interaction is not yet known.

As the substrate potential is moved to more negative values, the HDT is desorbed from the substrate and forms the insoluble structure described above and shown in Figure 3b. In this case, the force on approach becomes more repulsive, which is consistent with a stronger electrostatic interaction between the two surfaces. In this case, there is no hydrophobic interaction between thiols assembled on the tip and thiolates in solution near the substrate to counteract the repulsive electrostatic interaction between the two arising from the desorbed thiolate trapped in the interaction region. This raises the effective concentration of the anion in the region between the tip and the sample and makes the force on approach repulsive, as expected.

4.1.3. Schematic Explanation during Desorption/Adsorption of HDT. Figure 7a shows schematic diagrams for the HDT-modified tip/substrate interaction. At the potential below the desorption peak, both tip and substrate are covered with HDT. In this case, F_{app} is repulsive and F_{ad} is large on retraction due to the thiol−thiol interactions. After HDT desorption from the substrate, thiolates remain in the interfacial region. The presence of disordered thiolates diminishes the magnitude of F_{ad} because most of the thiol−thiol interactions are no longer available. However, F_{app} becomes attractive, likely due to a hydrophobic interaction between the disordered thiolates on the surface and the ordered thiolates on the tip.

When the Au tip is not covered with thiols (Figure 7b), the potential dependent behavior is different from that described above. F_{ad} is small at the potentials below the desorption peak because the CH_3-CH_3 interactions are no longer available. F_{app} is repulsive likely due to electrostatic interaction. Following desorption of the HDT adlayer from the surface, F_{app} becomes more repulsive due to a more Au−Au like interaction, which is known to be repulsive in this potential region.

Finally, Figure 7c provides an explanation of the long-range F_{ad} observed when both the tip and substrate were held at −1.2 V for the HDT−HDT case. This effect can be explained in terms of the role of solvent.[1] We suggest that the bare Au−thiolate interaction is such that a bridge structure forms between tip and substrate without allowing water to wet the hydrophobic ends. Thus, when the substrate is retracted, these thiolates exert a force opposite to the tip movement and can show longer interaction distance than usual. This force results in retraction curves with a gradual and continuous pull-off instead of a jump-off-contact, as shown experimentally in Figure 3c.

4.2. ET-Modified Tip and Substrate. *4.2.1. Adhesion Measurements.* In contrast to HDT, ET is soluble in water. Additionally, the shorter chain length usually results in a SAM which is somewhat less ordered than that found with the longer chain lengths.[58,59] The interaction between the ET-modified Au substrate and the ET-modified AFM tip also showed a large F_{ad}. The magnitude of W_{ad} for the ET−ET interaction was found to be 67 ± 6 mJ/m^2 on the beginning of the cathodic scan and this magnitude was regained after a full potential cycle, as shown in Figure 4a. The decrease of W_{ad} compared to the HDT−HDT case is expected from the fact that the interaction energy would be function of contact angle, where thiols having small contact angles give rise to small interaction energy between thiols.[21]

Desorbing ET from the substrate led to a decrease in W_{ad} to a value of 6 ± 2 mJ/m^2, consistent with removal of dominant CH_3-CH_3 interactions. W_{ad} for the ET-modified tip and the ET-desorbed substrate is found to be much smaller compared to that for HDT case, where about $^1/_4$ of the total W_{ad} is retained after the desorption. This suggests that the strong interactions between thiols are no longer available as the substrate becomes free of ET. Ethanethiolate is known to be soluble in aqueous solution, and the desorbed thiolate are likely mostly diffused away into a bulk solution phase.[60] Comparable measurements for the bare Au−bare Au case revealed a nearly zero W_{ad} (0.4 ± 0.1 mJ/m^2), which suggests that some ET still remains in the interfacial region.

With an ET-desorbed bare Au tip and an ET-modified Au substrate (see Figure 5a), W_{ad} is again small and comparable to that found with the ET-covered tip and the ET-desorbed substrate. However, the adhesion force between bare Au tip and ET-modified Au substrate exhibits a very weak potential dependence. W_{ad} deceases gradually as the substrate potential goes to the negative end, and then regains its magnitude after a full potential cycle. When both tip and substrate are free of thiols, the magnitude of W_{ad} is almost zero (0.6 ± 0.2 mJ/m^2), suggesting that there is some limited participation of the ET in modifying the adhesion. However, this effect is small.

4.2.2. Approach Measurements. When both the Au tip and the substrate were covered with ET at −0.5 V, the force curve on approach exhibited almost zero interaction force at 5 nm before contact as shown in Figure 4b. This interaction is potential independent, which is likely a consequence of both the high ionic strength used and the relatively large potential drop known to occur within the thiolate film**.** The jump-to-contact occurred at a distance of 2∼3 nm, which is very large compared to the length scale of ET on the Au substrate.

Moving the potential through the desorption peak led to an increase in the jump-to-contact distance, which appears in Figure 4b as an attractive interaction on approach. This increase

undoubtedly reflects the instability in the area between tip and sample as ET desorbs from the tip and has some residence time within the interaction region. After ET is completely desorbed, F_{app} returns to near zero. Interestingly, the force curve no longer appears as a repulsive interaction at starting at ca. 3 nm off the substrate but rather exhibits no repulsive interaction until jump-to-contact. The tip−surface interaction now approximates much better the Au−Au interaction found above.

F_{app} between the bare Au tip and the ET-modified Au substrate exhibited a repulsive feature with no potential dependence as was found to be very close to zero at 5 nm off the surface. The behavior found here is very similar to that found for the Au−Au case and likely reflects development of the double layer very close to both electrode surfaces.

4.2.3. Schematic Explanation during Desorption/Adsorption of ET. The AFM force measurements with the ET-modified substrate showed somewhat different features compared to those with the HDT-modified substrate. Figure 8a shows schematic diagrams for the ET-modified tip/substrate interaction. At the potential below the desorption peak, it shows a repulsive feature as the tip is approached to the substrate and exhibits a large F_{ad} on retraction due to the thiol−thiol interactions. As the substrate potential reaches the desorption peak, the ET-modified substrate starts to be disordered and eventually desorbed from the substrate. As the substrate becomes more unpacked, the magnitude of F_{ad} would be reduced because most of the thiol−thiol interactions will not be available after the desorption. Because of high solubility of desorbed ethanethiolates, they would be diffused away from the substrate into the bulk solution, and eventually the bare Au substrate will emerge in the tip/substrate interaction region.

The overall interaction changes between the bare Au tip and ET-modified substrate during the desorption/adsorption are illustrated in Figure 8b. There is a small magnitude of F_{ad} at the potential below the desorption peak, because the substrate is fully covered with ET and the tip has a tiny amount of residual ET. As the substrate potential reaches the desorption peak, the ET-modified substrate starts to be disordered and eventually desorbed from the substrate. As the substrate becomes more unpacked and both the tip and substrate are free of the thiols adlayer, the magnitude of F_{ad} would be greatly reduced. Then the interaction would be very similar to bare Au-bare Au interaction.

4.3. Differences between the Different Thiol Chain Lengths. The AFM force measurements for HDT-modified and ET-modified substrate show that the interaction between the tip and the substrate can be varied depending upon the length of the thiol. The interaction between the HDT-modified tip and the substrate shows a strong potential dependence regardless of tip state, whereas the interaction between the ET-modified tip/substrate exhibits a weaker potential dependence, especially the interaction between the ET-desorbed tip and ET-modified substrate.

When both the tip and substrate are modified with thiols, the change of F_{ad} follows the voltammetric features. In the cathodic scan, both HDT and ET are desorbed from the substrate after passing the desorption peak. In the anodic scan for the ET-modified Au substrate, F_{ad} starts to increase after passing the anodic peak. However, in contrast to the HDT case, F_{ad} of the desorbed ET substrate does not reach its initial value until nearly at the positive potential limit. This contrasts with the strong potential dependence of the deposition of long-chain thiols, which is shown in the HDT-modified substrate results.

The change of F_{app} on the approach curve also shows the potential dependence behavior. The interaction between both the SAM-covered tip and the substrate showed strong repulsion in the short range due to the influence of the alkaline electrolyte of high concentration. When the SAM on the tip was removed in the cathodic scan, the strong repulsion disappeared and an attractive force was developed. The attractive force remained after the desorption in the HDT case; however, the attractive feature was removed and negligible right after passing the cathodic peak in the ET case.

It is known that the solubility of the adsorbates plays a role in the electrodeposition of thiolates; lower surface coverage and more distorted packing is observed when the oxidative adsorption is carried out in aqueous solvents where the solubility of thiolates is high.[59,60] The concentration of thiolates close to the surface may be large because the primary species present in solution would be ethanethiolates based on the estimated pK_a of ET (∼10.6).[61] However, the ethanethiolate is unlikely to form micelles since the solubility of ethanethiolates in aqueous solution is relatively large and the desorbed thiolates likely diffuse away from the substrate quickly, leading to a low concentration of ET in solution.

Conversely, it is easy to understand the strong potential dependence of HDT adsorption by assuming that the HDT will be better ordered than the ET during the adsorption process due to the longer chain length that stabilizes ordered structures in HDT. Another reason for the fast recovery for the HDT-modified substrate is that on the Au substrate fragments of the desorbed thiolates remain near the substrate after the desorption occurred. The reduced solubility of the HDT after desorption leads to the formation of a micellular structure above the electrode, which strongly influences subsequent force curve behavior.

V. Conclusions

AFM force measurements of the reversible desorption/adsorption of ET and HDT in the alkaline solution have been addressed. We demonstrated that the SAM-modified tip/substrate interaction showed the potential-dependent change. For the HDT-modified tip/substrate, the overall changes of the force curve corresponded well to its cyclic voltammogram. The adhesion interaction between the HDT-modified tip and the substrate showed the large F_{ad} that is matched with the JKR theory, whereas the adhesion was reduced to one-quarter of its original value after HDT on the substrate is removed. The attractive feature on approach curve and the relatively large F_{ad} on retraction after the desorption potential showed that the desorbed thiolates would be involved during force measurements. The interaction between the HDT-desorbed tip and the HDT-modified substrate also showed potential-dependent, and the tip/substrate interaction became more repulsive upon desorption and the F_{ad} showed long-range feature due to the formation of a bridge-like structure between desorbed thiolates.

We also showed that remarkably different interaction behaviors were obtained by changing the alkanethiol chain length. For the ET-modified tip/substrate, the overall interaction was matched well with its voltammetric feature with a similar fashion shown in the HDT-modified tip/substrate interaction. The interaction exhibited time-dependent recovery after the adsorption peak because the short chain thiols can diffuse away following the desorption and need to be brought to the substrate to reorganize to their initial state. However, the interaction showed little potential dependence when the ET-desorbed tip was interacted with the ET-modified substrate.

Acknowledgment. We thank Prof. Bruce Manning for helpful discussions. This work was funded by the NSF (CHE-02-37683), which is gratefully acknowledged.

References and Notes

(1) Israelachvili, J. N. *Intermolecular & Surface Forces*, 2nd ed.; Academic Press: New York, 1992.
(2) Takano, H.; Kenseth, J. R.; Wong, S.-S.; O'Brien, J. C.; Porter, M. D. *Chem. Rev.* **1999**, *99*, 2845.
(3) Cappella, B.; Dietler, G. *Surf. Sci. Rep.* **1999**, *34*, 1.
(4) Janshoff, A.; Neitzert, M.; Oberdorfer, Y.; Fuchs, H. *Angew. Chem., Int. Ed.* **2000**, *39*, 3212.
(5) Butt, H.-J. *Encyclopedia Electrochem.* **2003**, *1*, 225.
(6) Hillier, A. C.; Kim, S.; Bard, A. J. *J. Phys. Chem.* **1996**, *100*, 18808.
(7) Campbell, S. D.; Hillier, A. C. *Langmuir* **1999**, *15*, 891.
(8) Wang, J.; Feldberg, S. W.; Bard, A. J. *J. Phys. Chem. B* **2002**, *106*, 10440.
(9) Barten, D.; Kleijn, J. M.; Duval, J.; von Leeuwen, H. P.; Lyklema, J.; Cohen Stuart, M. A. *Langmuir* **2003**, *19*, 1133.
(10) Considine, R. F.; Dixon, D. R.; Drummond, C. J. *Langmuir* **2000**, *16*, 1323.
(11) Larson, I.; Drummond, C. J.; Chan, D. Y. C.; Grieser, F. *Langmuir* **1997**, *13*, 2109.
(12) stankovich, J.; Carnie, S. L. *Langmuir* **1996**, *12*, 1453.
(13) Melendres, C. A.; Bowmaker, G. A.; Leger, J. M.; Beden, B. *J. Electroanal. Chem.* **1998**, *449*, 215.
(14) Raiteri, R.; Margesin, B.; Grattarola, M. *Sens. Actuators, B* **1998**, *B46*, 126.
(15) Serafin, J. M.; Hsieh, S.-J.; Monahan, J.; Gewirth, A. A. *J. Phys. Chem. B* **1998**, *102*, 10027.
(16) Serafin, J. M.; Gewirth, A. A. *J. Phys. Chem. B* **1997**, *101*, 10833.
(17) Marti, A.; Haehner, G.; Spencer, N. D. *Langmuir* **1995**, *11*, 4632.
(18) Thomas, R. C.; Houston, J. E.; Crooks, R. M.; Kim, T.; Michalske, T. A. *J. Am. Chem. Soc.* **1995**, *117*, 3830.
(19) Kang, M.; Gewirth, A. A. *J. Phys. Chem. B* **2002**, *106*, 12211.
(20) Skulason, H.; Frisbie, C. D. *Langmuir* **2000**, *16*, 6294.
(21) Sinniah, S. K.; Steel, A. B.; Miller, C. J.; Reutt-Robey, J. E. *J. Am. Chem. Soc.* **1996**, *118*, 8925.
(22) Noy, A.; Vezenov, D. V.; Lieber, C. M. *Annu. Rev. Mater. Sci.* **1997**, *27*, 381.
(23) Ulman, A. *Chem. Rev.* **1996**, *96*, 1533.
(24) Poirier, G. E. *Chem. Rev.* **1997**, *97*, 1117.
(25) Schwartz, D. K. *Annu. Rev. Phys. Chem.* **2001**, *52*, 107.
(26) Nuzzo, R. G.; Allara, D. L. *J. Am. Chem. Soc.* **1983**, *105*, 4481.
(27) Weisshaar, D. E.; Lamp, B. D.; Porter, M. D. *J. Am. Chem. Soc.* **1992**, *114*, 5860.
(28) Zhong, C.-J.; Porter, M. D. *J. Electroanal. Chem.* **1997**, *425*, 147.
(29) Ma, F.; Lennox, R. B. *Langmuir* **2000**, *16*, 6188.
(30) Kawaguchi, T.; Yasuda, H.; Shimazu, K.; Porter, M. D. *Langmuir* **2000**, *16*, 9830.
(31) Wong, S.-S.; Porter, M. D. *J. Electroanal. Chem.* **2000**, *485*, 135.
(32) Yang, D. F.; Al-Maznai, H.; Morin, M. *J. Phys. Chem. B* **1997**, *101*, 1158.
(33) Byloos, M.; Al-Maznai, H.; Morin, M. *J. Phys. Chem. B* **2001**, *105*, 5900.
(34) Vela, M. E.; Martin, H.; Vericat, C.; Andreasen, G.; Creus, A. H.; Salvarezza, R. C. *J. Phys. Chem. B* **2000**, *104*, 11878.
(35) Hobara, D.; Miyake, K.; Imabayashi, S.-i.; Niki, K.; Kakiuchi, T. *Langmuir* **1998**, *14*, 3590.
(36) Wano, H.; Uosaki, K. *Langmuir* **2001**, *17*, 8224.
(37) Byloos, M.; Al-Maznai, H.; Morin, M. *J. Phys. Chem. B* **1999**, *103*, 6554.
(38) Will, T.; Dietterle, M.; Kolb, D. M. *NATO ASI Series, Series E: Appl. Sci.* **1995**, *288*, 137.
(39) Hutter, J. L.; Bechhoefer, J. *Rev. Sci. Instrum.* **1993**, *64*, 1868.
(40) Senden, T. J. *Curr. Opin. Colloid Interface Sci.* **2001**, *6*, 95.
(41) Yang, D. F.; Wilde, C. P.; Morin, M. *Langmuir* **1997**, *13*, 243.
(42) Kakiuchi, T.; Usui, H.; Hobara, D.; Yamamoto, M. *Langmuir* **2002**, *18*, 5231.
(43) Tormoen, G. W.; Drelich, J.; Beach, E. R., III. *J. Adhes. Sci. Technol.* **2004**, *18*, 1.
(44) van der Vegte, E. W.; Hadziioannou, G. *Langmuir* **1997**, *13*, 4357.
(45) Warszynski, P.; Papastavrou, G.; Wantke, K. D.; Mohwald, H. *Colloid Surf. A* **2003**, *214*, 61.
(46) Strbac, S.; Hamelin, A.; Adzic, R. R. *J. Electroanal. Chem.* **1993**, *362*, 47.
(47) Strbac, S.; Adzic, R. R. *J. Electroanal. Chem.* **1996**, *403*, 169.
(48) Li, Y. Q.; Tao, N. J.; Pan, J.; Garcia, A. A.; Lindsay, S. M. *Langmuir* **1993**, *9*, 637.
(49) Dunstan, D. E. *Langmuir* **1992**, *8*, 738.
(50) Kekicheff, P.; Marcelja, S.; Senden, T. J.; Shubin, V. E. *J. Chem. Phys.* **1993**, *99*, 6098.
(51) Dicke, C.; Haehner, G. *J. Phys. Chem. B* **2002**, *106*, 4450.
(52) Kokkoli, E.; Zukoski, C. F. *J. Colloid Interface Sci.* **1999**, *209*, 60.
(53) Freitas, A. M.; Sharma, M. M. *J. Colloid Interface Sci.* **2001**, *233*, 73.
(54) Smith, C. P.; White, H. S. *Anal. Chem.* **1992**, *64*, 2398.
(55) Boubour, E.; Lennox, R. B. *Langmuir* **2000**, *16*, 7464.
(56) Vericat, C.; Andreasen, G.; Vela, M. E.; Martin, H.; Salvarezza, R. C. *J. Chem. Phys.* **2001**, *115*, 6672.
(57) Li, J.-H.; Yang, C.-H.; Yan, J.-C.; Chen, W.-Q.; Dong, S.-J. *Chin. J. Chem.* **1997**, *15*, 130.
(58) Laibinis, P. E.; Nuzzo, R. G.; Whitesides, G. M. *J. Phys. Chem.* **1992**, *96*, 5097.
(59) Esplandiu, M. J.; Hagenstroem, H.; Kolb, D. M. *Langmuir* **2001**, *17*, 828.
(60) Schneider, T. W.; Buttry, D. A. *J. Am. Chem. Soc.* **1993**, *115*, 12391.
(61) Hatchett, D. W.; Stevenson, K. J.; Lacy, W. B.; Harris, J. M.; White, H. S. *J. Am. Chem. Soc.* **1997**, *119*, 6596.